UNITED NATIONS UNIVERSITY
UNU-GTP
Geothermal Training Programme

Orkustofnun, Grensasvegur 9,
IS-108 Reykjavik, Iceland

Reports 2014
Number 32

GEOCHEMICAL STUDIES OF GEOTHERMAL FLUID AND EVALUATION OF WELL TEST RESULTS FROM WELLS SM-01, SM-02 AND SM-03, SOL DE MAÑANA FIELD, GEOTHERMAL PROJECT, LAGUNA COLORADA, BOLIVIA

Daniel Gustavo Villarroel Camacho
Empresa Nacional de Electricidad (ENDE)
Av. Ballivián N°503, Cochabamba
BOLIVIA
daniel.villarroel@ende.bo, danielg.villarroel@gmail.com

ABSTRACT

ENDE (National Electricity Company of Bolivia) carried out well testing of wells SM-01, SM-02 and SM-03 in the geothermal field Sol de Mañana in 2013, twenty six years after they were drilled. Temperature, pressure and spinner logging were carried out under static (non-flow) and discharging conditions. The flow rates and enthalpies were measured using the Russell James and TFT methods and the results obtained showed a good correspondence between the two methods. According to the steam flow obtained by TFT, wells SM-01, SM-02 and SM-03 may generate 7, 7.8 and 8.2 MWe, respectively. Samples of brine and steam were collected during discharge through each of the four orifice plates used during the tests. Samples for silica analysis were not properly preserved. Calculations based on silica concentrations, such as reservoir concentrations, and temperatures, based on geothermometers, were not reliable due to silica polymerization. A Na/K geothermometer was in agreement with temperatures obtained from logs. Ternary diagrams of cations and anions showed a reservoir temperature of 280°C and classifies the fluid as mature water. Amorphous silica is expected to form at 150°C and 4.8 bar-a. The calcite solubility curve showed an uncommon behaviour, perhaps due to unreliable pH values. A mineral called Teschemacherite (NH_4HCO_3) was observed in well SM-02. Teschemacherite is a possible cause of the clogging of well SM-05. A special approach was performed in order to determine the scaling potential of Teschemacherite but, unfortunately, the necessary thermodynamic information was not available.

1. INTRODUCTION

1.1 Location and description

Bolivia is located in the centre of South America between the meridians 57°26´- 69°38´western longitude and 9°38´- 22°53´ southern latitude. The South American tectonic plate is bordered by the Nazca and Antarctic plates to the west. These three plates meet at the Chile triple junction, and Bolivia is located above the subduction of the Nazca Plate. Bolivia is divided into the Andes to the west and

Amazon land to the east. The Bolivian Andes are comprised of three main ranges: Cordillera Occidental to the west (on the border with Chile), Cordillera Central, and Oriental to the east.

In addition to these mountain ranges, the Altiplano plateau extends over a large area between the Cordillera Occidental and the Cordillera Central. The plateau is around 700 km long and has a maximum width of approximately 200 km. The average elevation is close to 3.750 m a.s.l.

1.2 Geology

The geothermal field of Sol de Mañana is located in the Cordillera Occidental in the southwest part of Bolivia, close to the triple border of Bolivia-Chile-Argentina. The rocks exposed at the surface were formed principally during the Tertiary and Quaternary periods (SERGEOTECMIN, 1996), as shown in Figure 1.

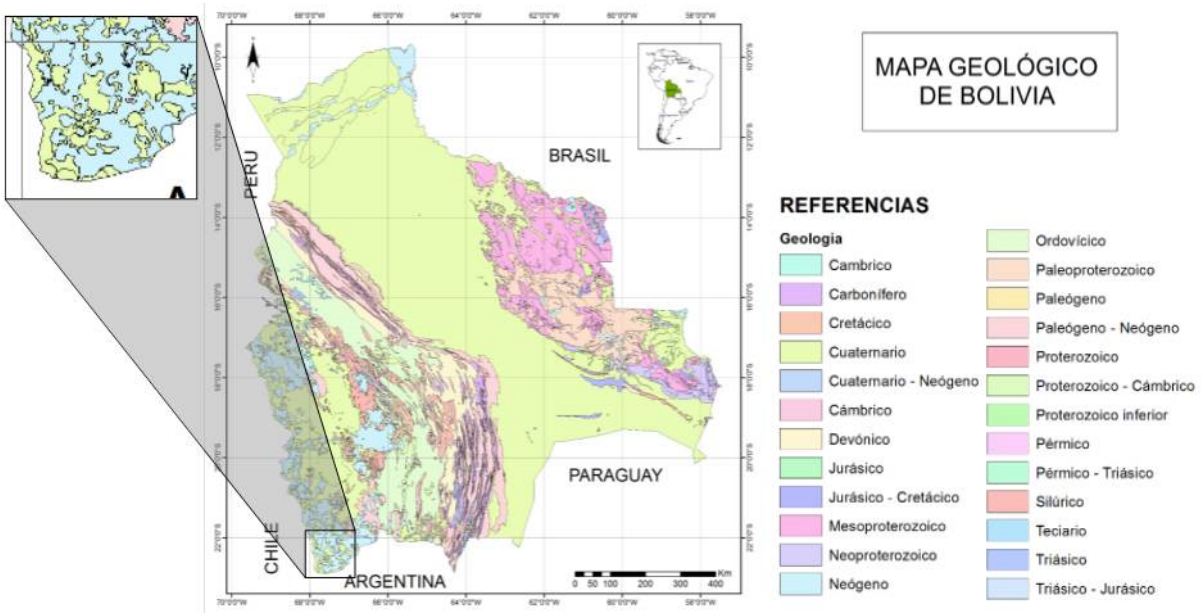

FIGURE 1: Geological map of Bolivia, with emphasis on the area of geothermal field Sol de Mañana (SERGEOTECMIN, 1996)

2. BACKGROUND

ENDE (National Electricity Company) and GEOBOL (Bolivian Geological Survey) started geothermal development in Bolivia in the 1970s with a reconnaissance study in Cordillera Occidental of the Western Andes Mountains which constitute the border with Chile. Forty two major geothermal manifestations have been studied and it was concluded that there are significant geothermal potential in the southwest region (GEOBOL, 1976).

In 1976, ENDE and the Ministries of Energy and Hydrocarbons, with funds from the United Nations Development Programme – UNDP, began evaluating Bolivian geothermal potential, based on the study by GEOBOL. Seven prospective geothermal areas were identified: Volcán Sajama, Empexa, Salar de la Laguna, Volcán Ollague-Cachi, Laguna Colorada, Laguna Verde and Quetena. Three of the seven fields were considered the most promising: Laguna Colorada, Sajama, and Valle de Río Empexa. They are located along the Occidental Cordillera of the Andes.

From 1978 to 1980, ENDE carried out a prefeasibility study for geothermal power plant construction in Laguna Colorada[1]. In 1989, a technical-economic evaluation was done, considering the installation of a 30 MW_e plant (ENDE, 1989).

In 1988, the government of Italy, through ENEL, and with technical cooperation of YPFB (Bolivian Oil Company), drilled the first geothermal well in Bolivia: Apacheta – 1. Wells SM-01, SM-02, SM-03 and SM-04 were drilled from 1988 to 1989. All of these wells produced steam except for well SM-04. However, well SM-04 has good permeability and could be used as an injection well. Well production varies between 350 and 370 t/h of geothermal fluid (steam and brine). Temperature and pressure logs indicated a reservoir temperature of 250-260°C and 30-48 bar, respectively (Villarroel, 2014).

From 1991 to 1992, ENDE deepened the reinjection well SM-04 from 1474 to 1726 m, and drilled production well SM-05. Unfortunately, due to a change in the political situation, the project was suspended in 1993.

From 1996 to 1997, ENDE contracted the Engineering Services of CFE of México to define the potential of the geothermal resources. CFE´s study confirmed that the minimum potential of the field is 100 MWe. CFE concluded that the potential of the field is 120 MWe for 25 years, with the development of 20 production wells and 7 reinjection wells, for approximately 4400t/h of brine (CFE, 1997).

In 2010, Japan International Cooperation Agency – JICA, and the government of Bolivia started discussions on the finances of the construction of a 50 MWe geothermal power plant in Sol de Mañana, based on feasibility studies of 100 MWe done in 2008 and 2010 by West – JEC. This study contains a conceptual model of the field (Figure 2) (West JEC, 2010).

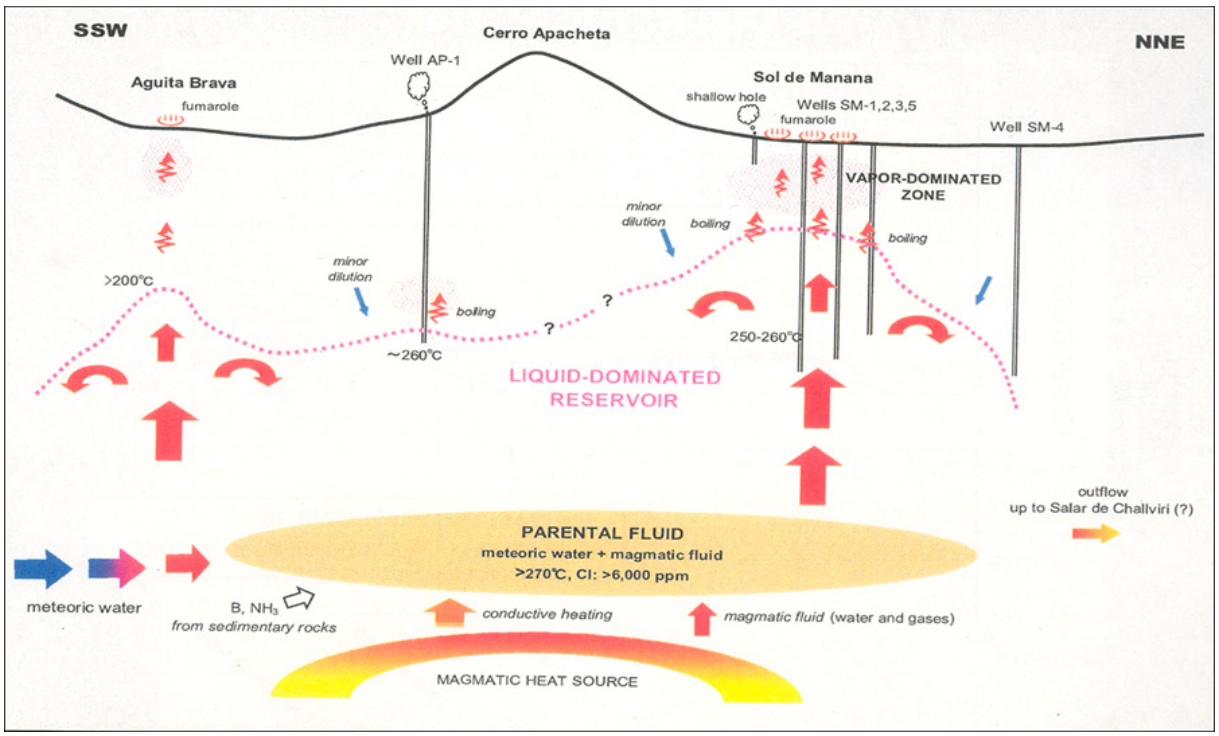

FIGURE 2: Conceptual model of geothermal field Sol de Mañana (West JEC, 2010)

[1] Laguna Colorada is not the geothermal field name, but just the representative name of the area where ENDE has its field camp. Sol de Mañana is the geothermal field´s name.

In May 2011, the project's preparatory phase (phase zero) started. Wells SM-01, SM-02, SM-03 were tested, and reinjection into well SM-04 was carried out from Nov. 2012 - May 2013. Due to an obstacle in well SM-05, it was not possible to log and test the well (Villarroel, 2014). An MT survey was carried out in early 2014 by Teranov and CGG. A resistivity profile from SSW to NNE is shown in Figure 3.

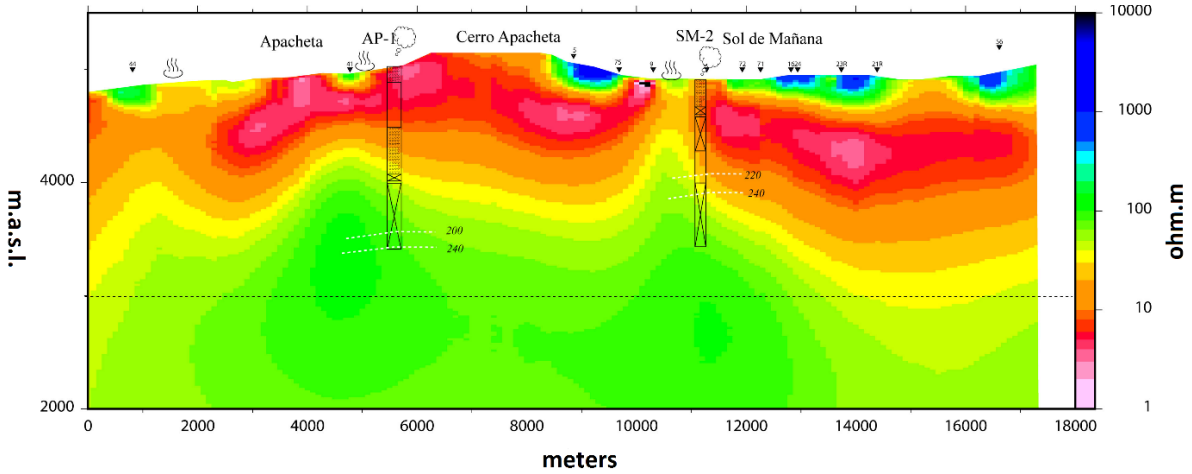

FIGURE 3: Resistivities in a SSW-NNE cross-section through the geothermal system Sol de Mañana (Teranov and CGG, 2014)

The data collected in phase zero is described and summarized in this report: well logs (temperature, pressure and spinner) in static and discharging conditions, different methods to measure the enthalpy and flow rate, evaluation and interpretation of the geochemical data, and estimation of possible scaling with emphasis on Teschemacherite (NH_4HCO_3) which was found in well SM-02, calcite and amorphous silica.Water from hot springs within the geothermal field has been monitored since 2011 in order to identify baseline conditions. The monitoring points LCN-1, LCN-2, LCN-3 and LCN-4 are located north of the project site, close to Laguna Colorada and the points Challviri, Polques I and II are situated at the east part of the field (Figure 4).

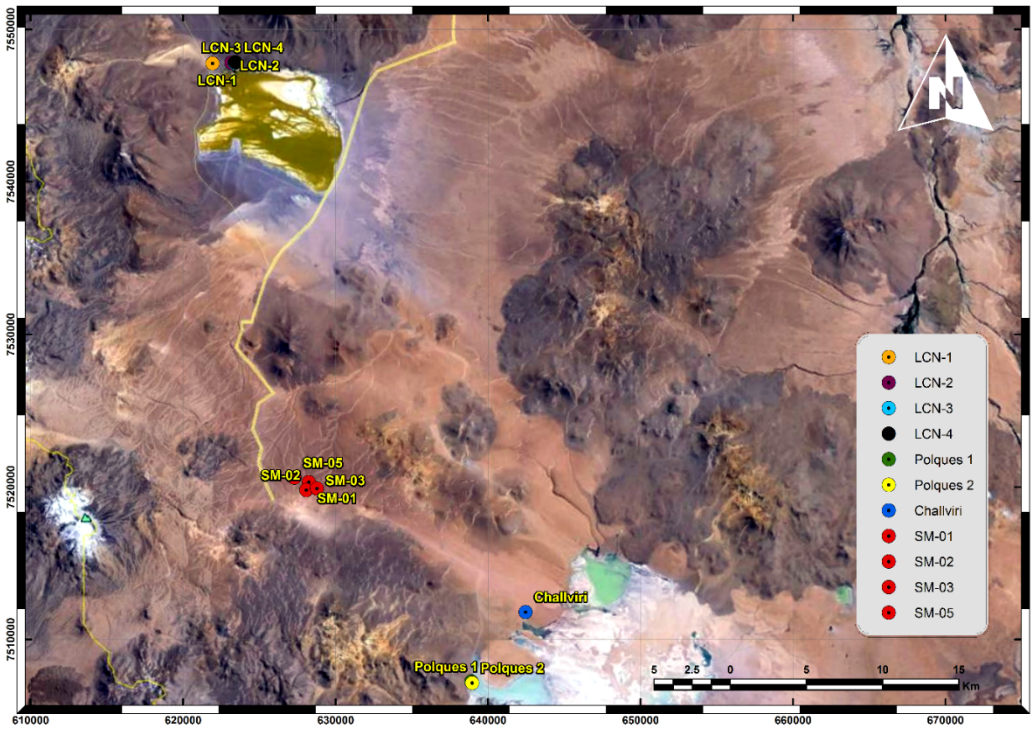

FIGURE 4: Location of monitoring points and Wells SM-01-SM-05

3. CHEMICAL CHARACTERISTICS OF DISCHARGE FROM WELLS SM-01, SM-02 AND SM-03

3.1 Status of the wells

3.1.1 Drilling history of well SM–01

The production well SM-01 was drilled in 1988 to a depth of 1180 m. The geological formations which the well passed through are considered to be of one main lithotype that is an ignimbrite of dacite composition with variable colours. The ignimbrite consists of quartz, plagioclase, biotite and hornblende, immersed in a vitreous matrix with a chaotic texture. Study of drill cuttings revealed three distinct hydrothermal alteration zones:

- Heulandite zone: 0 - 400 m;
- Quartz – chlorite zone: 400 - 780 m; and
- Epidote zone: 780 – 1180 m.

Quartz is stable at temperatures above 180°C (Franzson et al., 2003) and epidote appears at temperatures above 250°C (Franzson et al., 2008).

In general, the logged temperature corresponds to the hydrothermal mineralogical associations. The continuous increase in temperature downwards to the top of the reservoir (230 – 240°C) and the absence of significant losses of circulation suggests conductive conditions in the upper part of the well. An isothermal profile at the end of the well suggests a convective reservoir with an appreciable permeability.

The temperature logs clearly showed a temperature gradient of 20-35°C/100 m and a variation temperature of 230 – 240°C from 977 m to the bottom of the well. The pressure at 1000 m depth was 43 bar. An injection test, carried out when the well had reached a depth of 1180 m, showed values of 2.8 $m^3 \cdot h^{-1} \cdot bar^{-1}$ (ENEL, 1989a).

3.1.2 Drilling history of well SM -02

The drilling of production well SM-02 started in 1988 and was completed in 1989 at 1486.5 m depth. The strata in the upper part are characterized by dacitic ignimbrites, followed by dacitic lavas. Dacitic ignimbrites are found in the deeper part of the well. The study of secondary minerals shows four hydrothermal alteration zones:

- Clay minerals zone: 0 – 400 m;
- Wairakite zone: 525 – 800 m;
- Wairakite-epidote zone: 800 – 900 m; and
- Epidote- adularia zone: 950 – 1486.5 m.

Wairakite appears at temperatures close to 200°C (Steingrímsson et al., 1986) and epidote appears at temperatures above 250°C (Franzson et al., 2008).

The well crossed some low-absorption capacity formations between 810 and 1200 m, partial losses at 920 m and total loss of circulation at 1486.5 m, where an injectivity test revealed an index of 67 $m^3 \cdot h^{-1} \cdot bar^{-1}$ (ENEL, 1989b).

3.1.3 Drilling history of well SM-03

The production well SM-03 was drilled in 1989 down to 1406 m depth. The strata are characterized by formations of dacitic ignimbrites from the top to 970 m depth. No cuttings were returned from greater

depth due to total loss of circulation. It was possible to distinguish three zones of hydrothermal alterations:

- Clay minerals zone: 0 – 500 m;
- Quartz - chlorite zone: 500 – 705 m; and
- Epidote zone: 705-977 m.

Quartz is stable at temperatures above 180°C (Franzson et al., 2003) and epidote appears at temperatures above 250°C (Franzson et al., 2008).

The injectivity reaches 26.9 $m^3 \cdot h^{-1} \cdot bar^{-1}$ at the bottom. The temperature logs showed a thermal gradient of 20-25°C/100 m with variations of 98.2 – 186.61°C between 315-734 m depth (ENEL, 1990).

3.2 Logs of wells SM-01, SM-02 and SM-03

Temperature and pressure logging are normally carried out in order to locate feed zones, to study flow between feed zones, estimate the magnitude (permeability) of individual feed points and estimate formation temperatures. The temperature distribution in geothermal systems is determined by heat and fluid flow (water and steam) through the system.

The estimation of the formation temperature is the first step to understand how the system works and to setting up a conceptual model (Steingrímsson, 2013). The temperature profile also permits a simple definition of reservoir properties: 1) when rock is impermeable, heat is transported by conduction; the profile showed a gradient in function on the thermal conductivity of the rock; 2) when rock is permeable, heat transported is by convection; the profile shows an isothermal curve (Grant and Bixley, 2011).

Pressure is an essential parameter in geothermal reservoir studies. This property controls fluid flow in the reservoir. Logging is carried out in order to: study well conditions (fluid flow, boiling, etc.); map reservoir pressures; study transient pressure variations due to fluid injection or production; monitor long term pressure changes due to exploitation. Global pressure variations in the reservoir are the driving force for fluid flow; time variations of the pressure reflect changes in the flow pattern and the fluid reserve of the reservoir (Steingrímsson, 2013).

Temperature and pressure logs were carried out in static and discharging conditions, using electronic geothermal tool K-10. Spinner logs were also collected for discharging conditions. Due to an obstacle inside well SM-05, it was not possible to conduct logs in that well.

3.2.1 Well logs in static conditions

The temperature and pressure logs in static conditions in wells SM-01, SM-02 and SM-03 were collected on December 5th, 4th and 3th 2012, respectively. The logs are shown in Figure 5; a comparison of the pressures and temperatures at 900 m depth is shown in Table 1:

TABLE 1: Measurements of pressure and temperature at 900 m depth for wells SM-01, SM-02 and SM-03 at static conditions

Well	Pressure [bara]	Temperature [°C]
SM-01	32.9	238.7
SM-02	26.9	230.4
SM-03	31.7	235.4

According to Figure 5, the water levels in static (no-flow) conditions are located at 850, 700 and 530 m depth for wells SM-01, SM-02 and SM-03, respectively. At these points, the pressure (constant from initial level) shows a gradient in function of the water density.

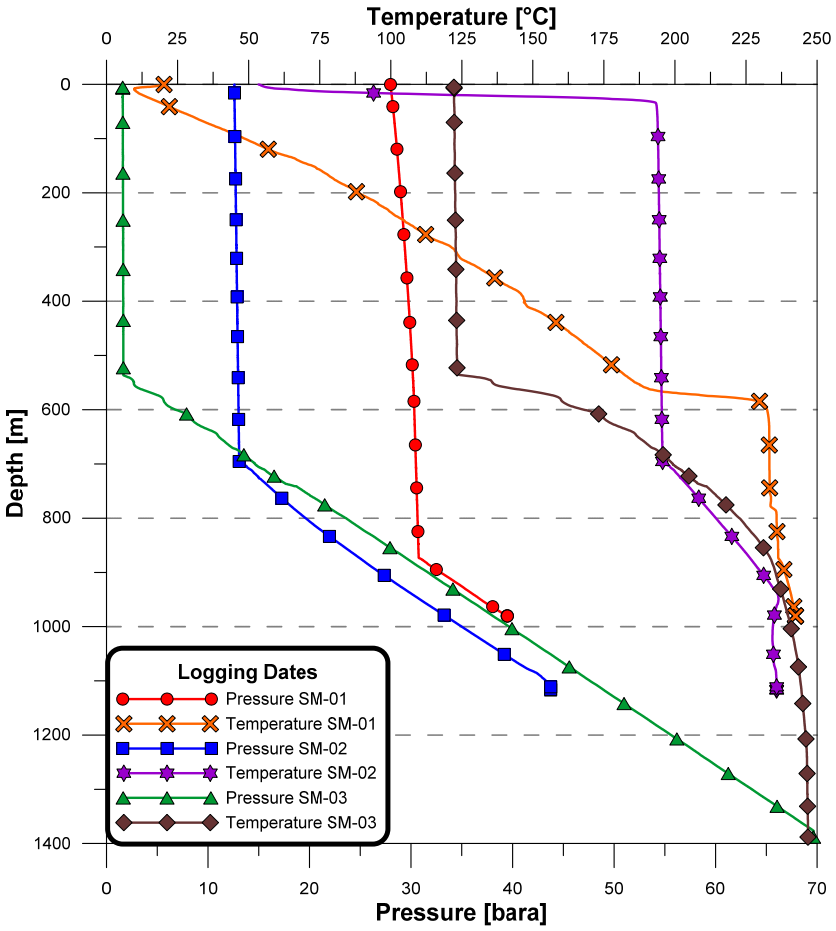

FIGURE 5: Temperature and pressure logs in static conditions for wells SM- 01, SM-02 and SM-03

Well SM-01 shows an increase in temperature from 20 to 180°C in the first 550 m; at this depth, the temperature increases suddenly to 230-235°C which is interesting as the water table is not reached until at ~900 m depth. From 600 to 1000 m, the temperature remains almost constant at this value. From surface down to 500 m, the temperature gradually increases from 25 to 185°C, possibly due to the presence of gases in this part of the well.

Well SM-02 shows a rapid increase in temperature until it reaches 185°C in the uppermost 50 m and remains constant down to the water table at 700 m depth. The low temperature in the uppermost 50 m is possibly due to the presence of gases. At 700 m, the temperature increases with a gradient of 20°C/100 m until it reaches approximately 235°C. Finally, an isothermal gradient was registered from 970 to 1150 m (235°C).

Well SM-03 shows a constant temperature between 0-530 m depth where a positive change in the gradient occurs, as does the pressure log at the same depth. Temperature remains constant at 250°C when it reaches 1200-1400 depth.

3.2.2 Well logs in discharging conditions

Production testing of well SM-01 was performed in December 2012. In order to evaluate the production well in different operating conditions, four orifice plates (2, 4, 6 and 10 inches) were used during the test. Unfortunately, the logs for the 10 inch orifice plate are not available for this well. The temperature, pressure and spinner logs are shown in Figure 6a.

The logging tool reached 1000 m depth in well SM-01. The temperature profile (Figure 6a) did not show drastic changes during the log and presented the same profile for each orifice plate. The temperature at 1000 m was 249°C. The same behaviour was observed in the pressure profiles. Pressure reached 40 bar at the same depth. The spinner graph showed the same behaviour for 4 and 6 inch orifice plates but registered lower values for the 2 inch orifice plate.

The testing of well SM-02 was carried out in April 2013. Orifices plates of 2, 4, 6 and 10 (completely open) inches in diameter were used during the test. Unfortunately, logs during discharge through the 10 inch orifice plate are not available.

The logging tool reached 1250 m depth in well SM-02. The temperature profile (Figure 6b) did not show drastic changes until at 1050 m where an isothermal behaviour was observed for each orifice plate. The temperature measured at 1250 m was 250°C. The same behaviour was observed in the pressure profile. The spinner graph showed the same behaviour for 4 and 6 inch orifice plates but registered low values for the 2 inch orifice plate.

Finally, testing of well SM-03 was performed in February 2013, using the same sized four orifices plates mentioned above (Figure 6c). The temperature profile remained constant from 950 to 1300 m with a measured temperature of 247°C. The spinner logs indicated inflow in the region below 1250 m depth.

3.3 Description and comparison of two methods used to determine flow and enthalpy

3.3.1 Russell James method

The lip-pressure method is a relatively economical and convenient method for measuring two phase flows, such as in geothermal wells, due to its advantages of simplicity in both hardware and instrumentation, and its ability to accommodate relatively large flows with less expensive test equipment. The technique is based on an empirical formula developed by James (1966) and is also based upon measurements made in wells with a low content of non-condensable gas or dissolved solids (Kruger and Ramey, 1978).

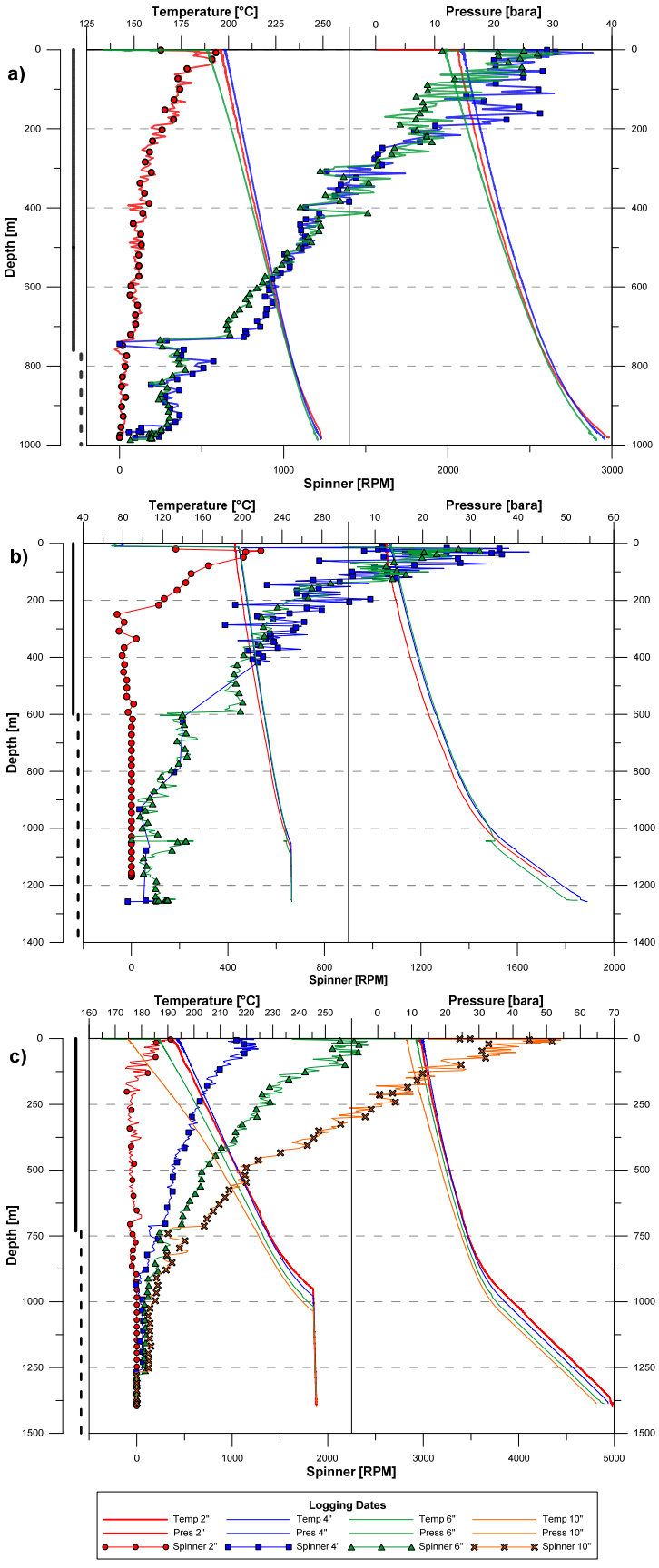

FIGURE 6: Temperature, pressure and spinner logs for wells (a) SM-01, (b) SM-02 and (c) SM-03 in discharging conditions

When the geothermal fluid is discharged to the atmosphere, it reaches sonic velocity on its way into an atmospheric pressure separator (or silencer). The lip pressure is measured at the expansion chamber, installed between the discharge pipeline and the silencer. Equation 1 relates mass flow, enthalpy and lip pressure as follows (Grant and Bixley, 2011):

$$\frac{G \times H^{1.102}}{P^{0.96}} = 663 \tag{1}$$

where G = W/A;
W = Mass flow [$T \cdot h^{-1}$];
A = Cross-sectional area of the pipe [cm^2];
H = Enthalpy of the mixture [$kJ \cdot kg^{-1}$];
P = Lip pressure [bara].

The separated water flow is readily measured in a weir box or manifold installed behind the silencer. The equation to relate the total flow and the enthalpy is given by Equation 2:

$$W = W_{wa} \frac{h_{sa} - h_{wa}}{h_{sa} - H} \tag{2}$$

where W = Total flow [$T \cdot h^{-1}$];
W_{wa} = Flow of liquid measured in the manifold [$T \cdot h^{-1}$];
Has = Enthalpy of steam at atmospheric pressure [kJ·kg];
h_{wa} = Enthalpy of liquid at atmospheric pressure [kJ·kg];
H = Enthalpy of the mixture [kJ·kg].

The average atmospheric pressure in Sol de Mañana is 567 mbar.

Then, in order to solve Equations 1 and 2 simultaneously, the iteration starts with an arbitrary value of total enthalpy and calculates the total flow in both cases; the iteration finishes when the values of total flow are highly similar to a specific enthalpy value.

3.3.2 Tracer flow test method

Tracer flow testing (TFT) procedures are increasingly becoming the standard method for flow testing wells at operating geothermal power plants. The method allows for on-line testing of the wells, avoiding disruptions to power station operations and the need for dedicated well test facilities (Grant and Bixley, 2011).

The TFT procedure involves the quantitative injection, at precise rates, of relatively small amounts of chemical tracers (for steam and brine) into the discharge line of the production wells. The dilution of tracers depend on the flow rate, i.e. the higher the flow, the lower the concentration. At some distance downstream, steam and brine are sampled and analysed for the tracers. Sampling points must be far enough downstream from the injection point in order that the tracer becomes fully mixed with the two phase flow (Lovelock, 2006).

Equations 3 and 4 are used to calculate liquid and vapour phase flow rates (Grant and Bixley, 2011):

$$W_w = \frac{W_T}{C_{TW} - C_{BW}} \tag{3}$$

$$W_V = \frac{W_T}{C_{TV} - C_{BV}} \tag{4}$$

where W_W = Mass flow rate of liquid phase;
W_T = Tracer injection mass flow rate;
W_V = Mass flow rate of vapour phase;
C_{TW} = Concentration of tracer in liquid phase by weight;
C_{BW} = Background concentration of tracer in liquid phase;
C_{BV} = Background concentration of tracer in vapour phase.

The TFT method also permits the calculation of the enthalpy, when the flow rates of liquid and steam and the conditions of sampling are known.

3.3.3 Results of flow measurements

Well testing was carried out between December 2012 and April 2013. Testing of wells SM-01, SM-02 and SM-03 was performed in December, April and March, respectively, and every well was monitored for one month (approximately one week per orifice plate); the results of the measurements of the flow rate and enthalpy are listed in Table 2.

In order to measure the sonic velocity of the fluid, an expansion chamber was installed at the end of the pipeline ahead of the silencer. A pressure gauge was installed into the expansion chamber to measure the lip pressure. Additionally, a weir box was installed behind the silencer in order to determine the flow rate of the separated brine.

The TFT method was carried out using a fluorescent and SF6 as liquid and steam tracers, respectively. The samples of brine and steam were collected in Webre separators installed 15-20 m past the injection point. In order to determine the concentration of the tracers in the brine and steam samples, a fluorimeter and electron capture detector (ECD) equipment were used, respectively.

TABLE 2: Results of flow rate measurements and enthalpy calculations, using the Russell James method and TFT method

Well	OP [inch]	WHP [barg]	Russell James method			TFT method				MWe[b]
			Total Flow [T/h]	Enthalpy [kJ/kg]	Steam Flow [T/h][a]	Pres. Sep. [bara]	Total Flow [T/h]	Enthalpy [kJ/kg]	Steam Flow [T/h]	
SM – 01	2	14.3	43.2	1160.1	15.2	2.2	48.0	1075.2	12.3	1.7
	4	15.0	159.4	1076.2	50.1	6.8	166.7	1130.8	35.3	4.9
	6	12.2	251.5	1120.0	83.9	7.3	243	1064.9	42.4	5.9
	10	10.7	289.0	1112.6	95.5	8.7	285.7	1099.8	51	7
SM – 02	2	13.2	41.1	1102.9	13.4	1.9	38.8	1067.9	10.2	1.4
	4	14.4	145.7	1088.0	46.6	7.3	148.8	1166.8	33.4	4.6
	6	11.4	237.7	1091.8	76.4	5.6	234.6	1069.2	46	6.4
	10	9.6	283.7	1092.8	91.3	6.0	288.1	1075.9	56.2	7.8
SM – 03	2	12.7	38.1	1186.6	13.8	1.9	-	-	-	-
	4	13.5	146.7	1071.3	45.8	7.0	-	-	-	-
	6	11.7	208.7	1058.5	64.0	8.7	-	-	-	-
	10	8.9	270.0	1068.6	84.0	4.6	274.1	1083.7	59.1	8.2

[a] Calculations take into account the flow of brine measured in a weir box.
[b] Calculations from the steam flow obtained with TFT method and the assumption: It takes about 2 kg/s of high pressure steam (7 bar-a) to generate 1 MW of electric power in high-efficiency turbines (Steingrímsson, 2014).

The results of the enthalpy and flow rate are similar, with variations of less than 7% and 5%, respectively.

3.4 Chemical composition of brine and steam

Brine and steam samples were collected during the discharge tests. The samples were collected using a webre separator, connected to the two phase pipeline, 15 m from the wellhead. Two phase samples were collected during discharge through each of the four orifice plates for each of the three wells. Samples for isotopic analysis of steam and brine and chemical analysis of condensate were collected, only while discharging through the 10 inch orifice plate. The analytical results for the 10 inch samples are shown in Table 3.

TABLE 3: Results of chemical analysis of brine and steam from wells SM-01, SM-02, SM-03

Chemical analysis of water separated			
Sample well	**SM-01**	**SM-02**	**SM-03**
Orifice Plate	10"	10"	10"
Date	1.01.13	25.04.13	23.02.13
WHP [bara]	10.8	9.5	8.9
P.Sep. [barg]	8.1	5.4	4
Na [mg/kg]	4060	4080	4310
K [mg/kg]	704	697	720
Ca [mg/kg]	206	192	219
Mg [mg/kg]	0.042	0.027	0.100
Li [mg/kg]	42.6	41.4	44.5
Sr [mg/kg]	3.92	3.64	3.94
Ba [mg/kg]	0.392	0.372	0.251
Fe [mg/kg]	<0.05	<0.05	0.224
B [mg/kg]	162	161	157
SiO_2 [mg/kg]	784	1330	619
Al [mg/kg]	0.284	0.032	0.104
Sb [mg/kg]	0.681	0.681	0.445
As [mg/kg]	27.4	27.9	33.1
Mn [mg/kg]	0.094	0.092	0.093
Cl [mg/kg]	7160	7100	7500
F [mg/kg]	3.8	4.07	4.03
Br [mg/kg]	6	5.94	6.14
SO_4^{-2} [mg/kg]	27.4	28.9	30.5
HCO_3^- [mg/kg]	22.9	30.7	<2
CO_3^{-2} [mg/kg]	<2	<2	<2
NH_4^+ [mg/kg]	2.1	1.97	2.27
CO_2 [mg/l]	16.5	22.1	<2
Iodide	<5	<5	<5
Cond. [umhos/cm]	22400	21900	22700
TDS (Calculated)	13200	13700	13600
Lab pH	6.98	7.12	4.32
δ^2H (%)	-82.7	-82.4	-91.7
$\delta^{18}O$ (%)	-6.77	-6.63	-9.76

Chemical analysis of steam condensate			
Sample well	**SM-01**	**SM-02**	**SM-03**
Orifice Plate	10"	10"	10"
Date	1.01.13	25.04.13	23.02.13
WHP [bara]	10.8	9.5	8.9
P.Sep. [barg]	7.7	5.0	3.6
B [mg/kg]	1.78	1.96	1.36
SiO_2 [mg/kg]	0.257	1.55	1.79
Cl [mg/kg]	0.681	17.6	4.67
Cond. [umhos/cm]	89.2	136	116
Lab pH	7.25	6.71	6.55
δ^2H (%), H_2O	-9.41	-10.15	-6.51
$\delta^{18}O$ (%), H_2O	-88.6	-91.8	-82.1

Chemical analysis of NCG[a]			
Sample well	**SM-01**	**SM-02**	**SM-03**
Orifice plate	10"	10"	10"
Litres Gas/Kg condensate	0.39	0.41	0.36
Sample Gas/Steam Ratio [mg_{gas}/kg_{steam}]	656	701	565
CO_2 [% v/v]	85.2	88.3	78.0
H_2S [%v/v]	8.13	6.06	7.6
NH_3 [%v/v]	4.1	3.6	3.86
Ar [%v/v]	0.011	0.00859	0.0127
N_2 [%v/v]	2.26	1.75	1.55
CH_4 [%v/v]	0.338	0.282	0.173
H_2 [%v/v]	<6.4	<2.18	8.8

CBE%	1.08	1.82	2.16

[a] Gas concentrations in volume percent of dry gas.

Samples for silica analysis were not properly preserved when collected. The silica analyses were carried out in two ways: The samples were acidified to pH 2 with nitric acid and analysed; this way was called "as received". However, due to silica polymerisation, a considerable amount of silica precipitated. Sodium hydroxide was added to the remaining sample fractions until pH 12 was reached before it was heated to 100°C for about 40 minutes; this way was called "digested". Table 3 shows only values for silica "digested". For these reasons, the calculations which used silica concentrations, e.g. geothermometers, were not reliable.

A significant variation was observed between the pH measured during the sampling and the pH issued by the laboratory, 7.31 at 8.6°C and 4.32 at lab temperature (20-25°C), respectively, for well SM-03. These pH and silica variations could be related as silica polymerization may change the pH of water

samples in two ways: by formation of oligomers that tend to decrease pH, and by removal of monomeric silica (weak acid) that tends to increase pH (Karingithi et al., 2010). Unfortunately, there are no pH field values for other wells to confirm that theory, and it was not possible to compare with the pH analysed in the laboratory. As the pH values are important in chemical modelling, this may have caused inaccuracies in the models/calculations discussed in this report.

While sampling the water phase, it is a common procedure to try to avoid possible degassing effects from the bottles, especially for the analysis of pH. Degassing is associated with loss of CO_2, and the concentration of CO_2 in the samples is highly related to the carbonate species (H_2CO_3, HCO_3^-, CO_3^{-2}). In this regard, if a sample is degassed, the pH tends to decrease. In order to avoid these issues, it is always recommended to measure the pH as soon as possible. The liquid samples from wells SM-01, SM-02 and SM-03 were not properly preserved and the pH measurements were carried out many days after the samples were collected. Thus, it is possible that degassing may have affected the pH measurements.

All the results issued by the laboratory are shown in Table 3, as well as the sampling conditions and wellhead pressure. The chemical speciation program WATCH (Bjarnason, 2010) was used to calculate the composition of the reservoir liquid and scaling potential. The WATCH program considered an atmospheric pressure of 1013 mbar. The input data were corrected, as the average atmospheric pressure in the field is 567 mbar (5000 m a.s.l.).

Table 4 shows the concentrations of the components in the reservoir, as calculated by the WATCH program at reservoir temperatures of 249, 250 and 247°C for wells SM-01, SM-02 and SM-03, respectively. The ion activity and solubility product constants, Q and K, for some minerals were obtained from the WATCH program. Scaling potential will be discussed in Chapter 3.7. However, it is necessary to mention that the calculations indicated a calcite oversaturation in the reservoir. The most likely explanation is the lack of accurate pH values. The saturation state was corrected and re-calculated in order to obtain corrections for the pH value. The calculated pH was 6.33 and 6.01 for wells SM-01 and SM-02, respectively; it was not necessary to make a correction in the pH for well SM-03.

TABLE 4: Calculated composition of the reservoir liquid from wells SM-01, SM-02 and SM-03, assuming reservoir temperatures of 249, 250 and 247°C, respectively

	SM-01	**SM-02**	**SM-03**
B [mg/kg]	134.54	128.90	124.00
SiO_2 [mg/kg]	651.09	1064.79	488.88
Na [mg/kg]	3371.7	3266.4	3404.0
K [mg/kg]	584.65	558.02	568.65
Mg [mg/kg]	0.035	0.022	0.079
Ca [mg/kg]	171.08	153.71	172.96
F [mg/kg]	3.156	3.258	3.183
Cl [mg/kg]	5946.2	5684.2	5923.4
SO_4 [mg/kg]	22.75	23.14	24.09
Al [mg/kg]	0.236	0.026	0.082
Fe [mg/kg]	0.000	0.000	0.177
TDS [mg/kg]	10962.2	10968.2	10741.1
CO_2 [mg/kg]	116.1	148.9	107.3
H_2S [mg/kg]	7.56	6.97	8.09
NH_3 [mg/kg]	3.65	3.65	3.85
H_2 [mg/kg]	0.00	0.00	0.56
O_2 [mg/kg]	0.00	0.00	0.00
CH_4[mg/kg]	0.15	0.15	0.09
N_2 [mg/kg]	1.73	1.65	1.36
pH	5.08	5.76	5.27

All the calculations were performed using these pH corrected values. Dramatic changes in the concentrations of the components and/or species, e.g. the values of the Charge Balance Error (CBE), were not observed.

The CBE was calculated using Equation 5:

$$CBE(\%) = \frac{\sum z_{cat} m_{cat} - \sum z_{an} m_{an}}{2[\sum z_{cat} m_{cat} + \sum z_{an} m_{an}]} \cdot 100\% \quad (5)$$

where z_i = Charge of cation or anion I;
m_i = Molal concentration of i [mol/kg].

When the value of CBE is less than 10%, the analysis of samples can be considered complete; the most representative compounds have been taken into account for the analysis.

Table 4 shows the concentration of the components at reservoir conditions, while the temperature was obtained from the logs (Section 3.2). The concentrations are similar between the wells with some exceptions, such as silica (discussed above), aluminium and iron. However, it is necessary to continue sampling and chemical analysis in order to confirm the values.

3.5 Classification of thermal waters

The most common type of fluid found at depth in high-temperature geothermal systems is with near-neutral pH, with high chloride concentrations compared to the anions. However, other types of water can be derived from geothermal fields, owing to chemical or physical processes. (Nicholson, 1993).

In this sense, the representation of the concentrations of the principal anions and cations are useful in order to classify the types of waters. In this report, the diagrams Cl-HCO_3-SO_4 and Na-K-Mg were used in order to classify the waters.

3.5.1 Cl-SO_4-HCO_3 Ternary diagram

The Cl-SO_4-HCO_3 ternary diagram is commonly used to classify geothermal fluids on the basis of the major anion concentrations. The plot aids in identifying the various water types, and assists in recognizing waters which are most suitable for geothermometry. The construction of the triangular graph result is relatively easy; the relationships between the anions are given by Equation 6 (Nicholson, 1993):

$$\sum Anion = C_{Cl} + C_{SO4} + C_{HCO3} \quad (6)$$

$$\%Cl = \frac{C_{Cl}}{\sum Anion} 100 \quad ; \quad \%SO_4 = \frac{C_{SO4}}{\sum Anion} 100 \quad ; \quad \%HCO_3 = \frac{C_{HCO3}}{\sum Anion}$$

where C_x = Concentration of the species [mg·kg^{-1}].

Bicarbonate represents the total concentration of all carbonate species in the water. According to the location of the points on the graph, the fluid can be classified into the following categories:

- **Mature waters**: These kinds of water contain high concentrations of chloride and are known as "alkali-chloride" or "neutral-chloride"; they are typical of the deep geothermal fluid found in most high-temperature systems where the pH is usually neutral. Chloride is used as a tracer in geothermal investigations because it is a conservative ion in geothermal fluids, as it does not take part in reactions with rocks after it has dissolved (Dolgorjav, 2009).
- **Peripheral waters**: Contains high concentrations of bicarbonates, possibly due to mixing with cold groundwater or can indicate the presence of carbonate rocks (Wei, 2006).

- **Steam heated waters:** The dominant cation is sulphate; these waters can originate from the condensation of geothermal gases into the liquid near the surface, but sometimes their origin can be related to equilibria deep down in the geothermal systems, and that may even be useful for interpretation. Although usually found near the surface at <100 m depth, sulphate waters can penetrate to depth through faults in the geothermal system. Since the concentration of silica and most cations is only the product of near-surface leaching, such steam-heated waters cannot be employed in geothermometry, as the concentrations of the dissolved constituents bear no relation to the mineral-fluid equilibria in the reservoir (Nicholson, 1993).

The Cl-SO_4-HCO_3 diagram for the geothermal fluid and the hot springs of Sol de Mañana field is presented in Figure 7.

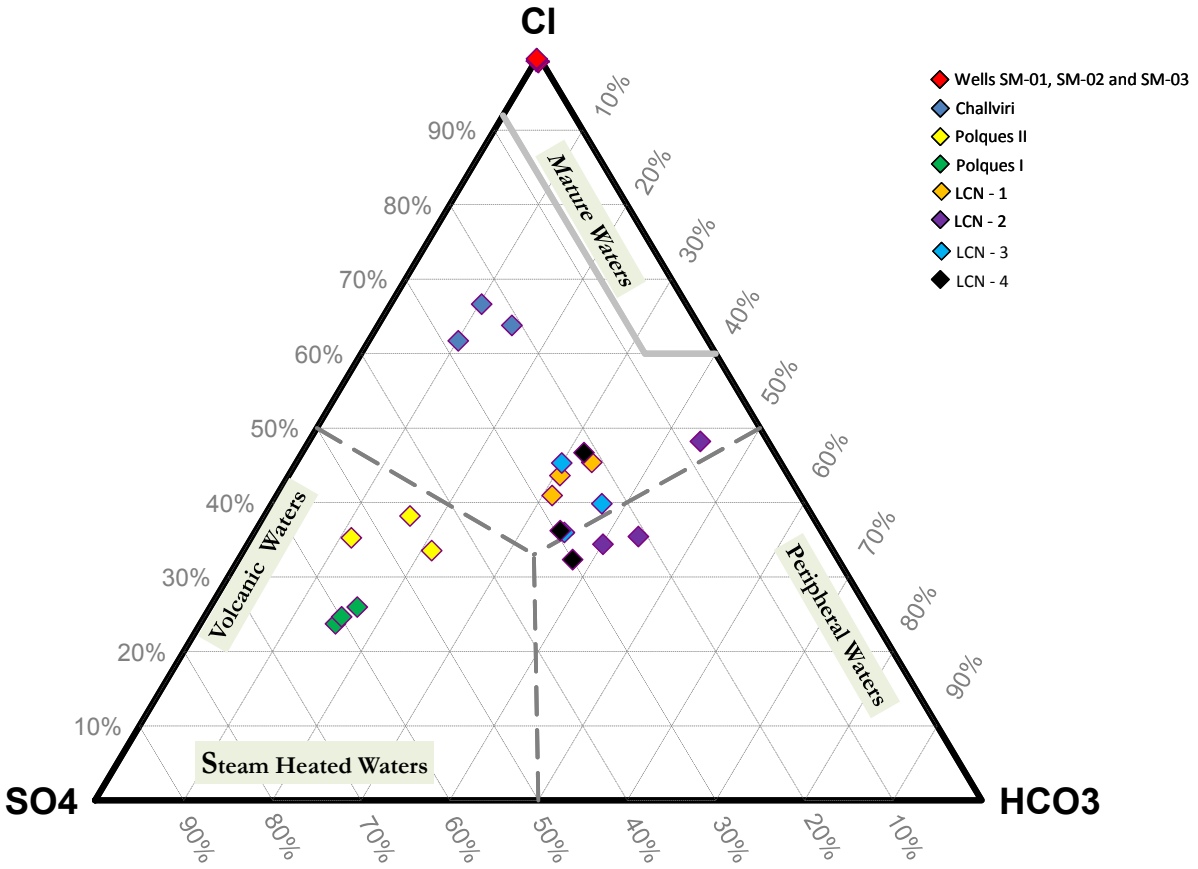

FIGURE 7: Cl-HCO_3-SO_4 ternary diagram for wells SM-01, SM-02, SM-03 and the hot springs of Sol de Mañana field

The points identifying the fluid from the wells are located in the chloride corner. It is common to observe this behaviour in high temperature systems with neutral pH. However, the issues with pH from these wells were explained in the previous section.

The points identifying the hot waters collected from surface manifestations (i.e. LCN-1, LCN-2, LCN-3 and LCN-4) show a similar concentration of the three species. These monitoring points are located around 30 km north of the geothermal field (Figure 4) and are not thought to be related to these waters. The hot water of LCN-1, LCN-2, LCN-3 and LCN-4 may postulate the presence of another heat source in Laguna Colorada.

Challviri shows a similar relationship of sulphate, comparative to the points of LCN, but different in chloride and carbonates. Polques I and II are the points with the highest relative content of sulphate. These manifestations may be influenced by the condensation of geothermal gases.

3.5.2 Ternary diagram Na-K-Mg

The Na-K-Ca ternary diagram is used to classify waters into fully equilibrated, partially equilibrated and immature waters, based on the relationships between these three cations, and can also determine reservoir temperature (geothermometer). In general, geothermometers can provide very good approximations when the water is fully equilibrated. The relationships between these cations are based on the following three reactions (Saudi, 1999):

The relationship between potassium and sodium is given by Equation 7 (Giggenbach, 1998):

$$\underset{\text{K-Feldespar}}{KAlSi_3O_8} + Na^+ \rightleftharpoons \underset{\text{Albite}}{NaAlSi_3O_8} + K^+ \quad (7)$$

The relationship between sodium and magnesium is given by: muscovite, clinochlore, silica and ion sodium with albite, k-feldspar, water and ion magnesium (Equation 8) (Giggenbach, 1998):

$$0.8KAl_3Si_3O_{10}(OH)_2 + 0.2Mg_5Al_2Si_3O_{10}(OH)_8 + 5.4SiO_2 + 2Na^+ \rightleftharpoons 2NaAlSi_3O_8 + 0.8KAlSi_3O_8 + 1.6H_2O + Mg^{2+} \quad (8)$$

And finally, the relationship between potassium and magnesium: muscovite, clinochlore, silica and ion potassium with k-feldspar, water and ion magnesium (Equation 9) (Giggenbach, 1998):

$$0.8KAl_3Si_3O_{10}(OH)_2 + 0.2Mg_5Al_2Si_3O_{10}(OH)_8 + 5.4SiO_2 + 2K^+ \rightleftharpoons 2.8KAlSi_3O_8 + 1.6H_2O + Mg^{2+} \quad (9)$$

This ternary diagram is constructed, based on these ion relationships. Points representing the liquid from the wells and hot springs are plotted in Figure 8.

According to Figure 8, the points representing the wells are plotted in the zone of full equilibration with a temperature of 280°C in the reservoir. The points representing liquid from LCN-1, LCN-2, LCN-3, LCN-4, Challviri, Polques I and II are plotted in opposite corners with a relatively high concentration of magnesium. Higher concentrations of magnesium can indicate near-surface reactions leaching Mg from the local rock, or dilution by groundwater (Nicholson, 1993).

3.6 Geothermometers

Geothermometers are a valuable tool in the evaluation and monitoring of geothermal reservoirs. It is based on mineral solubility, e.g. silica, exchange reactions Na-K, Na-K-Ca, etc. (see Chapter 3.5.2) and in gas mineral equilibria, such as CO_2, H_2, CO_2-H_2 and others (Arnórsson, 2000).

For a successful use of geothermometers, it is important to apply the following assumptions: the concentration of the elements or species is controlled only by a temperature-dependent mineral-fluid reaction; the reactions reach equilibrium in the reservoir; there is no mixing or dilution of the deep fluid; no near-surface reactions; and there is an abundance of the minerals and/or dissolved species in the rock-fluid system for the reaction to occur readily (Nicholson, 1993).

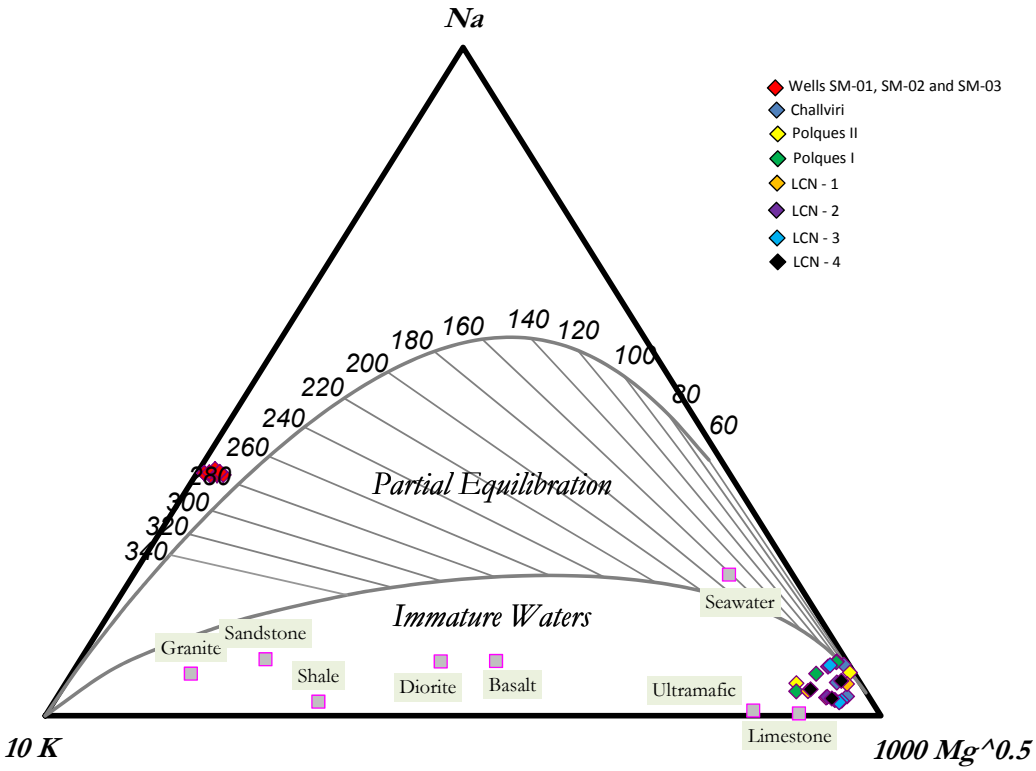

FIGURE 8: Na-K-Mg ternary diagram for wells SM-01, SM-02, SM-03 and the hot springs of Sol de Mañana field

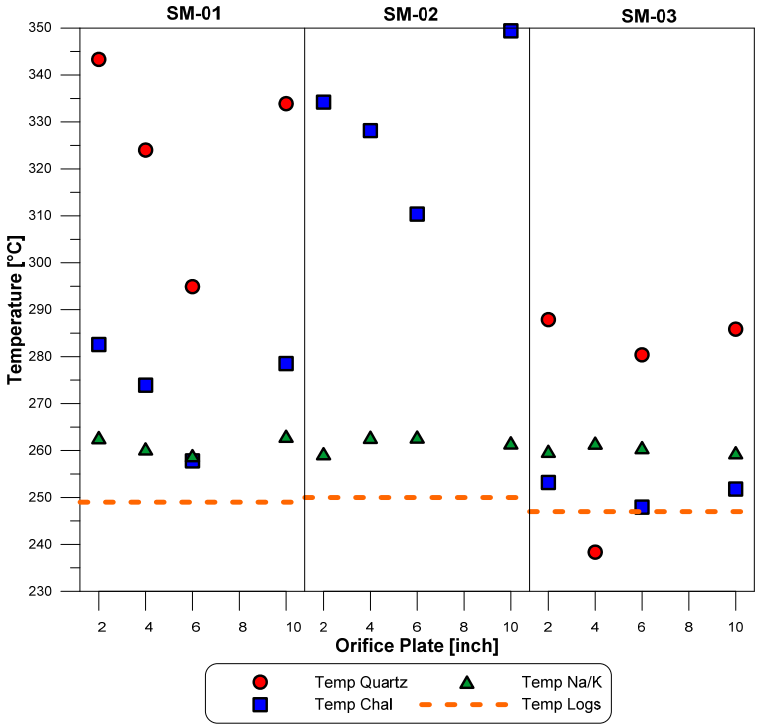

FIGURE 9: Comparison between calculated temperature based on quartz, chalcedony and Na/K geothermometers and logs for wells SM-01, SM-02 and SM-03; Quartz temperature was not plotted for well SM-02 due to shown values of more than 370°C

3.6.1 Water geothermometers

Theoretically, any cation ratio and any uncharged aqueous species concentration can be used as a geothermometer, as long as equilibrium prevails. In this way, many geothermometers have been studied and applied since the last century. Currently, silica (quartz and chalcedony), Na-K and Na-K-Ca are the most important geothermometers. Figure 9 shows a comparison between the measured reservoir temperature in wells SM-01, SM-02 and SM-03 and calculated temperatures based on quartz, chalcedony and Na/K geothermometers. The equations used for the calculation of the geothermometers are given in Table 5.

Temperatures based on quartz and chalcedony (silica) are not in agreement with the temperature measured, due to silica polymerisation, but a considerable

amount of silica precipitated during the transport of the samples to the laboratory, as was explained in Section 3.4. The digestion was performed in the remaining sample, after the first analysis (called "as received") (Section 3.4). Probably this explains the relatively high silica concentration and the high values of calculated temperature based on these geothermometers. According to Table 5, the relationship between silica and the temperature is direct.

TABLE 5: Geothermometer equations for liquid phase

Geothermometer	Equation (T°C)	Source
$T_{qtz,FP}$ $(SiO_2)^a$	$-42.2 + 0.28831S - 3.6686 \times 10^{-4}S^2 + 3.1665 \times 10^{-7}S^3 + 77.034 logS$	(1)
$T_{chal,AR}$ $(SiO_2)^a$	$\frac{1112}{4.91 - \log S} - 273.15$	(2)
$T_{Na/K,AR}$ $(Na/K)^b$	$\frac{1319}{1.699 + \log {Na}/{K}} - 273.15$	(3)

(1) Fournier and Potter (1982); (2),(3) Arnórsson et al. (1983)
[a] S is SiO_2 in [mg·kg^{-1}]. [b] Na/K in [mg·kg^{-1}]

However, the Na/K geothermometer shows a very stable relationship for all the wells in all the operating scenarios. The average temperature of 260°C is a very good representation of the temperature obtained in the logs.

3.6.2 Gas geothermometers

Gas geothermometers have been developed since the 1980s and, currently, their use is common around the world, especially when geological exploration is carried out and the ratios of steam/water, gas/steam and others are unknown (Arnórsson, 2000).

Figure 10 shows the temperature of gas geothermometers applied to the wells and the fumaroles located around the wells. The temperature, based on H_2S, has a good relationship with the temperature measured in the wells. However, for the fumaroles, the values were relatively high. The same happens with the temperature of CO_2; the values for wells SM-01 and SM-03 were not plotted, due to the very low values.

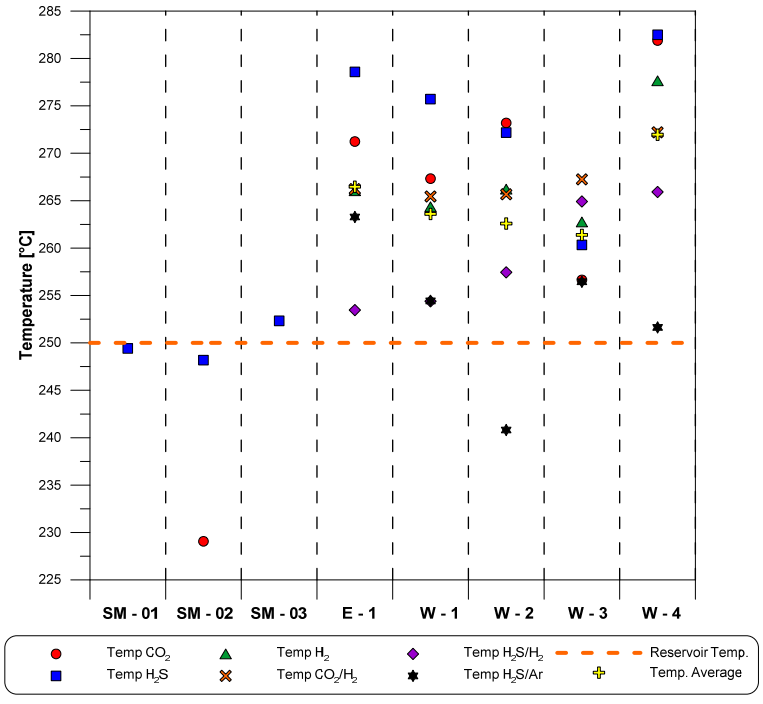

FIGURE 10: Comparison between reservoir and gas geothermometer gases for wells SM-01, SM-02, SM-03 and fumaroles points E-1, W-1-4, located on the geothermal field

In the case of fumaroles, the sensitivity of CO_2 and H_2S can be affect by condensation, boiling and dilution in the upflow below the manifestation. The use of geothermometers based on gas ratios removes such problems. The Argon concentration from an atmospheric source in the deep geothermal fluid is equal to that of air-saturated water (Arnórsson, 2000). The H_2S/Ar geothermometer gave a temperature close to the temperature of the reservoir. However, the average of all the geothermometers used in this

case present a value between 265 and 270°C. The Equations with which the geothermometers were calculated are shown in Table 6.

TABLE 6: Geothermometer equations of gases

Geothermometer	Equation (T°C)	Source
T_{CO2} $(CO_{2,g})^a$	$-44.1 + 269.25Q - 76.88Q^2 + 9.52Q^3$	(1)
T_{H2S} $(H_2S_{,g})^b$	$246.7 + 44.8Q$	(1)
T_{H2} $(H_{2,g})^b$	$277.2 + 20.99Q$	(1)
$T_{CO2/H2}$ $(CO_{2,g}/H_{2,g})^b$	$341.7 - 28.57Q$	(1)
$T_{H2S/H2}$ $(H_2S_{,g}/H_{2,g})^b$	$304.1 - 39.48Q$	(1)
$T_{H2S/Ar}$ $(H_2S_{,g}/Ar_{,g})^c$	$4.108Q^2 + 42.265Q + 137.6$	(2)

Q denotes the logarithm of the respective gas concentration or gas ratio log (mol·kg^{-1})
(1) Arnórsson and Gunnlaugsson (1985); (2) Arnórsson et al. (1998)
[a] For all waters; [b] All waters above 300°C and waters in the range 200-300°C for Cl>500 ppm. [c]Ar concentrations in geothermal reservoirs waters are equal to those in air-saturated water at 5°C

3.7 Speciation calculations and mineral saturation

As mentioned in Chapter 3.4, the WATCH program is a powerful tool used to describe the aqueous speciation distribution in the aquifer. WATCH has a thermodynamic database of some minerals (anhydrite, calcite, prehnite, wairakite, etc.). In order to determine possible scaling, the program allows the user to take into account different boiling steps for evaluation of the equilibrium state. The saturation state is evaluated by comparing the reaction quotient Q and the equilibrium constant of solubility K. Therefore, at equilibrium K=Q; for an under-saturated solution, Q<K, and for a super-saturated solution, Q>K (Arnórsson, 2000).

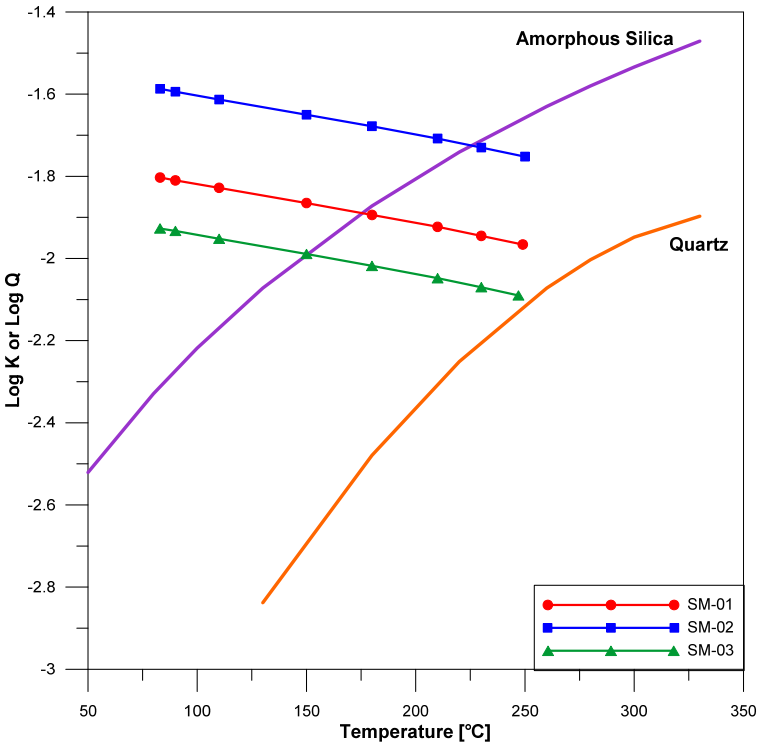

FIGURE 11: Reaction quotient Q for wells SM-01, SM-02 and SM-03 as a function of temperature; lines representing equilibrium of quartz and amorphous silica are shown with red and blue lines respectively.

The saturation index (SI = log Q/log K) was calculated for quartz-amorphous silica and calcite. A special approach was made for the solubility characteristic of Teschemacherite (NH_4HCO_3), a mineral which was found in well SM-02 and which is possibly the cause for the clogging of well SM-05.

Figure 11 shows the saturation index of silica, as a function of temperature assuming seven boiling steps from 230 to 83°C, this last one corresponding to the boiling temperature at the atmospheric pressure of the field. The boiling process assumed conservation of mass and enthalpy and the temperature at reservoir was taken from Section 3.2.2.

The aim of this graph is to evaluate the transition between the crystalline state of silica at

reservoir temperature and the temperature at which amorphous silica is expected to form and cause scaling inconveniences.

As was explained in Chapter 3.4, there were problems in the analysis of silica, presumably due to the effects of precipitation. Therefore, the reaction quotient Q will be not considered for wells SM-01 and SM-02 in the analysis of Figure 11, as the measured silica concentration does not correspond with the "real" reservoir conditions. Taking into account the value of Q for well SM-03, it is possible to predict silica scaling problems at 150°C and 4.8 bar-a. However, it is necessary to confirm this statement.

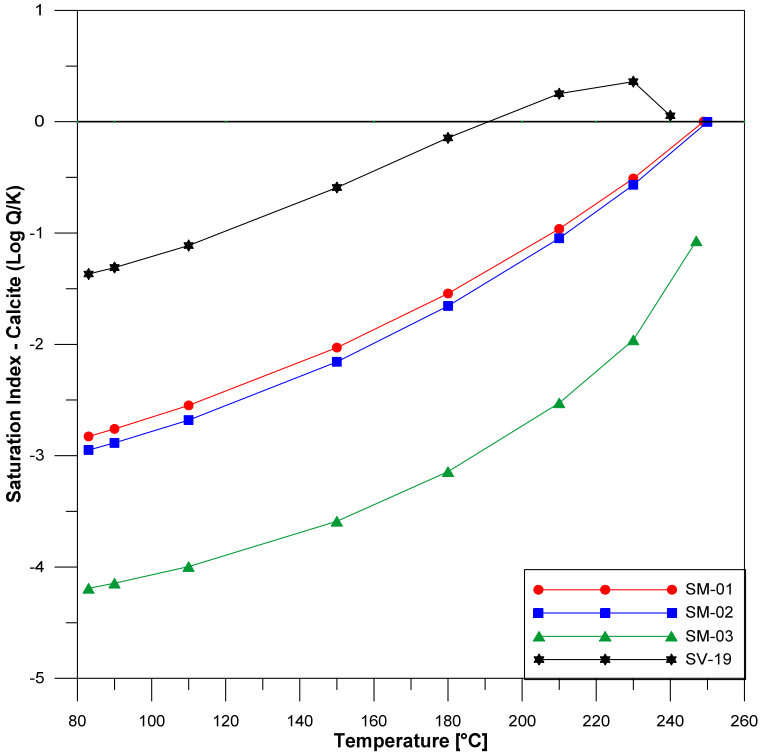

FIGURE 12: Saturation index of calcite for the wells of Sol de Mañana field and for well SV-19 of the Svartsengi geothermal field

In the same way, the analysis of calcite solubility was performed assuming seven adiabatic boiling steps, as was mentioned for evaluating silica. Figure 12 shows the saturation index as a function of temperature.

When the calculation of calcite solubility was performed, an unusual behaviour was noted. When the boiling starts, an increase of the log Q/K ratio of calcite is commonly observed before it decreases as the boiling continues. An example of such behaviour, based on a sample from well SV-19 in Svartsengi (Iceland) was also plotted. The analytical results from well SV-19 are shown in Appendix I. For calculation of the calcite saturation index from the wells of Sol de Mañana field, the pH assumptions are described in Section 3.4.

The pH is highly associated with concentrations of carbonate ions in the water (See Section 3.4.) and with the concentration of calcite. The concentrations of carbonates in a solution are directly proportional to pH; when the pH decreases, the concentration of calcite also decreases. This statement was confirmed when making variations in the pH values in WATCH program for wells SM-01 and SM-02.

3.7.1 Teschemacherite

Teschemacherite (bicarbonate of ammonia - NH_4HCO_3) is a mineral which was found during phase zero in well SM-02; it is presumably clogging well SM-05. Frederick Edward Teschemacher (1791-1863) was the first who described the mineral; its distribution in the world was found in Argentina, South Africa and on the Chincha and Guañapes Islands off the coast of Peru (Anthony et al., 2003).

The occurrence of Teschemacherite, inside the wellhead of the Broadlands geothermal drillhole BR 9 (New Zealand), is the only reference known describing this mineral (at the moment), in geothermal settings, encountered to date (Browne, 1972).

In order to define the curve of solubility (Saturation Index) for this mineral, Equations 10-12 of the reaction and the quotient Q are defined as follows:

$$NH_4HCO_3 \rightleftharpoons NH_4^+ + HCO_3^- \quad (10)$$

$$\log Q = \log a_{NH_4^+} + \log a_{HCO_3^-} \quad (11)$$

$$\log Q = \log(\gamma_{NH_4^+} \cdot [\,]_{NH_4^+}) + \log(\gamma_{HCO_3^-} \cdot [\,]_{HCO_3^-}) \quad (12)$$

where a = Activity;
γ = Activity coefficient;
[ ] = molar concentration.

The values of the concentration and coefficient of activity were obtained from WATCH, assuming the same seven adiabatic boiling steps mentioned in the sections above. The results are shown in Table 5.

TABLE 5: Values for quotient Q for wells SM-01, SM-02 and SM-03 at seven steps boiling

Temperature [°C]	**SM-01 log Q**	**SM-02 log Q**	**SM-03 log Q**
Temp. d.l.[a]	-9.106	-9.027	-10.21
230	-9.699	-9.624	-9.926
210	-9.780	-9.704	-10.09
180	-9.748	-9.678	-10.16
150	-9.674	-9.612	-10.15
110	-9.603	-9.557	-10.13
90	-9.596	-9.553	-10.14
83	-9.600	-9.557	-10.14

a: Temperature of deep liquid: 249, 250 and 247°C, respectively

The thermodynamic properties used for the calculation of the solubility constant of the equilibrium K, are shown in Table 6. Unfortunately, as it was not possible to obtain values of molar heat capacity at constant temperature, Cp, for the mineral, the calculation of SI could not be performed in this study.

TABLE 6: Thermodynamic properties for the ammonium cation, bicarbonate and teschemacherite (Wagman et al., 1982)

	$\Delta_f H°$ [kJ·mol^{-1}]	**$\Delta_f G°$ [kJ·mol^{-1}]**	**S° [J·mol^{-1}·K^{-1}]**	**Cp [J·mol^{-1}·K^{-1}]**
NH_4^+	-132.51	-79.31	113.4	79.9
HCO_3^-	-691.99	-586.77	91.2	
NH_4HCO_3	-849.4	-665.9	120.9	

4. CONCLUSIONS

The temperature and pressure logs and the chemical composition of the discharge from wells SM-01, SM-02 and SM-03 postulate the same reservoir temperature, the similar chemical composition and that they are hydrogeologically connected. These three wells presented an isothermal profile that indicates a convective system.

According to a Cl-SO_4-HCO_3 ternary diagram, the geothermal fluid could be classified as mature water of neutral pH with relatively high concentrations of chloride. A Na-K-Mg ternary diagram indicated a fully equilibrated reservoir liquid with a reservoir temperature of 280°C, whereas liquid from the hot springs in the area showed signs of mixing with cold groundwater.

Considering the diagram of silica scaling potential, amorphous silica is expected to precipitate at 150°C and 4.8 bar-a.

The temperature obtained from Na/K, H_2S, H_2S/Ar and H_2S/H_2 geothermometers is in agreement with the measured reservoir temperature. Geothermometers based on the silica concentration gave unreliable results, due to incomplete sampling procedures. For that reason, it is recommended to improve the sampling procedures and treatment, e.g. measure the pH in the field and carry out the analysis of H_2S, carbonates and others as soon as possible (preferably on the same day of sampling) and to dilute sample fractions used for silica analysis. Gas geothermometers based on the ratios of two components represent the temperature better than geothermometers based on one compound, suggesting a condensation or dilution in the fumaroles.

In order to determine future scaling problems, it is necessary to determine a value for the equilibrium constant (K) for teschemacherite.

ACKNOWLEDGEMENTS

I would like to thank the Government of Iceland and especially the United Nations University – Geothermal Training Programme for giving me a scholarship to take part in the six months course. Special gratitude goes to Mr. Lúdvík S. Georgsson and Mr. Ingimar G. Haraldsson for giving me the opportunity to participate in this course and for their support in completing this training.

Many thanks go to Ms. María Gudjónsdóttir, Ms. Thórhildur Ísberg and Mr. Markús Wilde for their assistance and training facilitation through the 6 months. Special thanks to Málfrídur Ómarsdóttir for her friendship, constant support and for being the best swimming teacher in the world.

I extend my gratefulness to my supervisors: Mr. Dadi Thorbjörnsson, for his guidance, patience, compromise and for sharing his vast knowledge and experience, and Mr. Thráinn Fridriksson, who is an excellent professor and friend; good luck in your new adventure, Thráinn! Special thanks go to Mr. Manabu Sugioka for believing in me.

Finally, thanks go to my parents and my brother for their huge love and comprehension and to God for showing me the correct way.

REFERENCES

Anthony, J.W., Bideaux, R.A., Bladh, K.W., and Nichols, M.C., 2003: Teschemacherite. In: Anthony, J.W., Bideaux, R.A., Bladh, K.W., and Nichols, M.C., *Handbook of mineralogy. V. Borates, carbonates, sulfates*. Mineralogical Society of America, Chantilly, VA, 791 pp, website: *www.handbookofmineralogy.org/pdfs/teschemacherite.pdf*

Arnórsson, S., 2000: *Isotopic and chemical techniques in geothermal exploration, development and use. Sampling methods, data handling, interpretation*. International Atomic Energy Agency, Vienna, 351 pp.

Arnórsson, S., and Gunnlaugsson, E., 1985: New gas geothermometers for geothermal exploration – calibration and application. *Geochim. Cosmochim. Acta, 49,* 1307-1325.

Arnórsson, S., Gunnlaugsson, E., and Svavarsson, H., 1983: The chemistry of geothermal waters in Iceland. II. Mineral equilibria and independent variables controlling water compositions. *Geochimica et Cosmochimica Acta*, 47, 547-566.

Arnórsson, S., Andrésdóttir, A., Gunnarsson, I., and Stefánsson, A., 1998: New calibration for the quartz and Na/K geothermometers – valid in the range 0-350°C (in Icelandic*). Proceedings of the Geoscience Society of Iceland Annual Meeting,* April, 42-43.

Bjarnason, J.Ö., 2010. *The speciation program WATCH* (vers. 2.4). ISOR – Iceland GeoSurvey, Reykjavík.

Browne, P.R.L., 1972: Occurrence of Teschemacherite in a geothermal well at Broadlands, New Zealand. *American Mineralogist, 57,* 1304-1305.

CFE, 1997: *Certification of potential of Sol de Mañana field, Bolivia.* CFE, internal report (in Spanish), submitted to ENDE, Bolivia.

Dolgorjav, O., 2009: Geochemical characterization of the thermal fluids from the Khangay area, central Mongolia. Report 10 in: *Geothermal Training in Iceland 2009.* UNU-GTP, Iceland, 125-150.

ENDE, 1989: *Geothermal power plant for Central Sol de Mañana, feasibility study for 30 MW*. ENDE, report (in Spanish).

ENEL, 1989a: *Geothermal feasibility study in the área of Laguna Colorada. Report of the well SM-01, BOL/84/007.*Empresa Nacional de Electricidad- ENDE, internal report (in Spanish), 111 pp.

ENEL, 1989b: *Geothermal feasibility study in the área of Laguna Colorada. Report of the well SM-02, BOL/84/007.*Empresa Nacional de Electricidad - ENDE, internal report (in Spanish), 179 pp.

ENEL, 1990: *Geothermal feasibility study in the area of Laguna Colorada. Report of the well SM-03.*Empresa Nacional de Electricidad - ENDE, internal report (in Spanish), 163 pp.

Fournier, R.O., and Potter, R.W. II, 1982: A revised and expanded silica (quartz) geothermometer. *Geoth. Res. Council Bull., 11-10*, 3-12.

Franzson, H., Zierenberg, R., and Sciffman, P., 2008: Chemical transport in geothermal systems in Iceland Evidence from hydrothermal alteration, *J. Volc. Geoth. Res*., *173,* 217-229.

Franzson, H., Gunnarsson, G., Danielsen, P., Sigurðsson, O., Hermannsson, G. and Skarphéðinsson, K., 2003: *Reykjanes - Well RN-13: Drilling report.* Orkustofnun, Reykjavik, report, OS-2003/030 (in Icelandic), 64 pp.

GEOBOL, 1976: *Geothermal resource evaluation for Bolivia.* Cochabamba, Bolivia, report (in Spanish).

Giggenbach, W.F. 1998: Geothermal solute equilibria. Derivation of Na-K-Ca geoindicators. *Geochim. Cosmochim. Acta, 52,* 2749-2765.

Grant, M.A, and Bixley, P.F., 2011: *Geothermal reservoir engineering* (2nd ed.). Elsevier, USA, 359 pp.

James, R., 1966: Measurements of steam-water mixtures discharging at the speed of sound to the atmosphere. New Zealand Engineering, 21-10, 437.

Karingithi, C.W., Arnórsson, S., and Grönvold, K., 2010: Processes controlling aquifer fluid compositions in the Olkaria geothermal system, Kenya. *J. Volcanol. & Geotherm. Res., 196-3/4,* 57-76.
Kruger, P., and Ramey, H. 1978: An evaluation of James´ empirical formulae for the determination of two-phase flow characteristics in geothermal wells. *Proceedings of the 4th Workshop on Geothermal Reservoir Engineering. Stanford University, Stanford, CA*, 7 pp.

Lovelock, B. 2006: Flow testing in Indonesia using alcohol tracers. *Presented at 31st Workshop on Geothermal Reservoir Engineering, Stanford University, Stanford, CA,* 5 pp.

Nicholson, K., 1993: *Geothermal fluids: chemistry and exploration techniques*. Springer-Verlag, Berlin, 268 pp.

Saudi, A.S.A.S., 1999: The Geothermal of thermal fluid in the geothermal field near Alia airport in Jordan and Selfoss geothermal field, S-Iceland. Report 13 in: *Geothermal training in Iceland 1999.* UNU-GTP, Iceland, 333-356 pp.

SERGEOTECMIN, 1996: *Geological map of Bolivia.* Servicio Nacional de Geología y Técnico de Minas, La Paz, Bolivia.

Steingrímsson, B., 2013: Geothermal well logging: temperature and pressure logs. *Presented at "Short Course on Conceptual Modelling of Geothermal Systems", organized by UNU-GTP and LaGeo, Santa Tecla, El Salvador,* 16 pp.

Steingrímsson, B., 2014: *Discharge measurement and injection tests.* UNU-GTP, Iceland, unpublished lecture notes, 64 pp.

Steingrímsson, B., Fridleifsson, G.Ó., Sverrisdóttir, G., Tulinius, H., Sigurdsson, Ó and Gunnlaugsson, E., 1986: *Nesjavellir, well NJ-15, drilling, investigations and production characteristics.* Orkustofnun, Reykjavik, report OS-86028/JHD-08 (in Icelandic), 119 pp.

Teranov and CGG (Compagnie Générale de Géophysique), 2014: *Geothermal project Laguna Colorada magnetotelluric survey Sol de Mañana.,* CGG, internal report submitted to ENDE, Bolivia.

Villarroel, D., 2014: Geothermal development in Bolivia. *Presented at "Short Course on Utilization of Low- and Medium-Enthalpy Geothermal Resources and Financial Aspects of Utilization", organized by UNU-GTP and LaGeo, Santa Tecla, El Salvador.* 6 pp.

Wagman, D., Evans, W., Parker, V., Schumm, R., Halow, I., Bailey, S., Churney, K., Nuttall, R., 1982: *The NBS tables of chemical thermodynamic properties. Selected values for inorganic and C1 and C2 organics substances in SI units*. J. Physical & Chemical Reference Data, USA, 407 pp.

Wei, W., 2006: Geochemical study of the Xianyang low-temperature geothermal field, Shaanxi Province, China. Report 22 in: *Geothermal training in Iceland 2006.* UNU-GTP, Iceland, 501-522.

West JEC, 2010: *Preparatory study for the geothermal development of Sol de Mañana, Bolivia.* West JEC, internal report (in Spanish), submitted to ENDE, Bolivia.

APPENDIX I: Laboratory analysis from well SV-19, Svartstengi – Iceland

Water sample (conc.:ppm)			**Steam sample (conc.:%)**	
pH/°C	7.92/25		Ar	1.5
B	7.8		CH_4	0.17
Ca	1130		H_2	3.02
Cl	14540		N_2	72.26
CO_2	8.9		O_2	23.06
F	0.21		CO_2 [mg/kg]	1600
K	1080		H_2S [mg/kg]	32
Mg	0.34			
Na	7320		*Physical and other data:*	
NH_3	0.71		Sample No.	20140186
SiO_2	479		Gas/steam [Lgas/kg condensate]	0.08
SO_4	26.7		Data sampling	8.5.2014
			Sampling pressure [bar-g]	12.8
			Sampling temperature [°C]	194.4